



Fermi/GBM observations of the ultra-long GRB 091024

D. Gruber¹, T. Krühler¹, S. Foley¹, M. Nardini¹, D. Burlon¹, A. Rau¹, E. Bissaldi¹,
A. von Kienlin¹, S. McBreen³, J. Greiner¹, and the *Fermi*/GBM collaboration.

¹ Max Planck Institute for extraterrestrial Physics, Giessenbachstrasse, Postfach 1312, D-85748, Garching, Germany

² University College, Dublin, Belfield, Stillorgan Road, Dublin 4, Ireland e-mail: dgruber@mpe.mpg.de

Abstract. We examine gamma-ray and optical data of GRB 091024, a gamma-ray burst (GRB) with an extremely long duration of $T_{90} \approx 1020$ s, as observed with the *Fermi* Gamma-Ray Burst Monitor (GBM). We present spectral analysis of all three distinct emission episodes using data from *Fermi*/GBM, and compare the optical and gamma-ray light curves of this event. We find that the optical light curve is highly anti-correlated to the prompt gamma-ray emission, with the optical emission reaching the maximum during an epoch of quiescence in the prompt emission. We interpret this behavior as the reverse shock (optical flash).

Key words. gamma rays: bursts ; gamma rays: observations;

1. Introduction

The *Fermi* Gamma-Ray Burst Monitor (GBM) (Meegan et al. 2009) was successfully launched on June 11, 2008. GBM observes the whole unocculted sky with a total of 12 sodium iodide scintillation detectors (NaI), sensitive between 8 keV to 1 MeV, and two bismuth germanate (BGO) detectors, covering an energy range from 200 keV to 40 MeV.

In this paper we present the gamma-ray observations together with already published optical observations of GRB 091024, a very long burst with a duration of approximately 1020 s. GBM triggered and located GRB 091024 at 08:55:58.47 (t_0) and triggered a second time at 09:06:29.36 UT (Bissaldi

& Connaughton 2009). *Swift*-XRT determined the position to be $\alpha_{J2000} = 22^h 37^m 00s$ and $\delta_{J2000} = 56^\circ 53' 21''$ with an uncertainty of 6 arcsec (Page & Marshall 2009). *Fermi* entered the South Atlantic Anomaly (SAA) 2830 s after t_0 , by which time GRB emission cannot be distinguished from the background.

Not many GRBs have been observed in the optical band while the prompt gamma-ray emission was still active (the best example being GRB 990123 and GRB 080319B, see e.g. Akerlof et al. 1999; Racusin et al. 2008). For GRB 091024 optical data were acquired soon after the first trigger, and throughout its active phase. Henden et al. (2009) obtained photometry using the Sonoita Research Observatory (SRO) starting 540 s after the trigger. Ten R_c -band, nine V -band, and one I_c -band

Send offprint requests to: D. Gruber

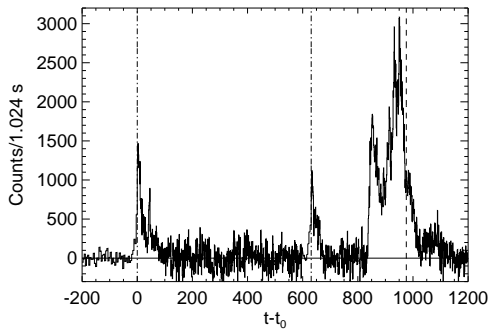


Fig. 1. Background corrected light curve of GRB091024 in the energy range 8 - 1000 keV. The vertical dash-dotted lines show the times of the two triggers and the dashed line the beginning of the autonomous repoint request (ARR).

exposures were acquired. The 2m - Faulkes Telescope North started observing the field of GRB 091024 207 s after the trigger (Cano et al. 2009). The 0.6m Super LOTIS telescope started observing 58 s after the BAT trigger (Updike et al. 2009).

2. GBM data analysis

Using all 12 NaI detectors, we created the background subtracted light curve shown in Fig. 1. It shows three distinct emission periods, separated by two periods of quiescence. The first emission episode consists of at least two FRED (Fast Rise, Exponential Decay) like pulses (hereafter episode I). Another emission episode starts 630 s after t_0 . This emission period, which actually triggered GBM a second time, consists of a single pulse (hereafter episode II). A multi-peaked episode starts 200 s later (corresponding to 840 s after t_0) and continues for 350 s (hereafter episode III). Because of the long-lasting phases of quiescence (630 s and 200 s, respectively), episodes I and II can be defined as precursors (Koshut et al. 1995; Lazzati 2005; Burlon et al. 2008).

Photons are detected up to ~ 500 keV during all three emission episodes. For the purposes of our spectral analysis we used CSPEC data (Meegan et al. 2009), from 8 keV to 40 MeV, with a temporal resolution of 1.024 s.

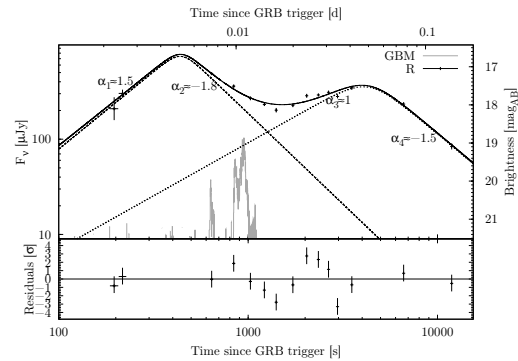


Fig. 2. Combined r-band light curve using data points from (Henden et al. 2009; Cano et al. 2009; Updike et al. 2009). The dashed line shows a reverse shock/forward shock modeling. The GBM light curve is presented in counts/s to guide the eye. *Swift*-XRT started observing 3000 s after the GBM trigger.

The spectral analysis was performed with the software package RMFIT (version 3.3rc8) and the GBM Response Matrices v1.8.

Three model fits were applied, a single power-law (PL), a power-law function with an exponential high-energy cutoff (COMP) and the Band function (Band et al. 1993). The best model fit is the function which provides the lowest Cash C-stat value (Cash 1979). The profile of the Cash statistics was used to estimate the 1σ asymmetric error.

For all three emission episodes the spectral fit was performed over the $T_{90,I}$ interval. The best fit spectral parameters are reported in Table 2.

3. Afterglow and optical flash

Using the data from (Henden et al. 2009; Cano et al. 2009; Updike et al. 2009) the gross behavior of the optical afterglow light curve is shown in Fig. 2.

The light curve has been fitted with the superposition of two different components. Each of these components is represented by a smoothly broken power law (Beuermann et al. 1999). Given the sparsely sampled data at $t < 600$ s, and the strong variability in the light curve there is considerable degeneracy

T-T ₀ [s]	E _p [keV]	α / index	C-Stat/DOF
-3.8 : 67.8	412 ⁺⁶⁹ ₋₅₃	-0.92 ± 0.07	740/479
622.7 : 664.7	371 ⁺¹¹¹ ₋₇₁	-1.17 ± 0.07	798/477
838.8 : 1070.2	278 ⁺²² ₋₁₈	-1.38 ± 0.02	1685/360

Table 1. Best fitting spectral parameters for the three emission episodes in GRB 091024. In all three intervals the COMP model was used.

between all fit parameters. We do reach, however, the following firm conclusions: The early optical light curve initially rises and peaks at around 450 s. Forcing the first peak to be simultaneous to the second emission episode in the GBM light curve $F_\gamma \propto t^\alpha$ at ~ 630 s results in a worse fit, and would require some fine-tuning of the parameters. Given that previous observations have shown the optical prompt emission to be quasi-simultaneous or somewhat later than the gamma-ray photons (Vestrand et al. 2005; Page et al. 2007; Krühler et al. 2009a), the first optical peak is therefore very likely unrelated to the emission seen in the GBM at 630 s. The initial afterglow rise-index α_1 is not well constrained by the data with a value of $\alpha_1 \approx 1.0 - 2.0$, which is compatible with what has been measured for previous rising afterglow light curves (e.g. Molinari et al. 2007; Panaitescu & Vestrand 2008; Krühler et al. 2009b; Oates et al. 2009). After the first peak, the first light curve component declines with an index of $\alpha_2 \approx -1.8$. This decay would be remarkably steep for a typical pre-jet break afterglow forward shock, but is consistent with the expectation for the decline of a reverse shock (Kobayashi 2000). We point out the possibility that such a steep decline could also be caused by a standard afterglow in a wind-like medium if assuming $p \approx 2.7$. Under the assumption that p remains constant throughout the afterglow, we use the *Swift*-XRT X-ray spectrum (Evans et al. 2007, 2009) between T0+3300 s and T0+50000 s, finding a spectral index of $\beta_X = 0.6 \pm 0.2$. Using the standard equations (see e.g. Zhang et al. 2006) we infer a value of $p = 2.2 \pm 0.4$ (for $\nu_m < \nu_X < \nu_c$) which is consistent with a wind-like medium within 90%. The second peak in the light curve could then be caused

for example by a refreshed shock, i.e. a late energy injection into the forward shockwave (e.g. Rees & Meszaros 1998), or by patchy shells which represent inhomogeneities in the angular energy distribution of the jet (e.g. Kumar & Piran 2000). However, the interpretation for a wind-like medium would require a much shallower rise ($\alpha \approx 0.5$, see Panaitescu & Vestrand 2008) than the one actually observed ($\alpha = 1.5$, see Fig. 2). Although we cannot rule out the possibility of a forward shock in a wind-like circum-burst medium, the light curve evolution argues against this scenario.

After the steep decay, the light curve reaches a temporary minimum at around 1200 s after which it rises again to a second peak at around 4000-5000 s. The light curve coverage is sparse around and after the second peak, but in any case the light curve peaks at a moment when there was no detection of further gamma-ray emission (*Fermi* was in the SAA at this time. However, *Swift*-BAT observed the field of GRB 091024 approximately 3000 s after the trigger and reported no detection). The second afterglow peak therefore is also unrelated to the prompt gamma-rays. Although sparsely sampled, the rise and the decay indices are consistent with the decay index of a typical afterglow forward shock.

Due to the lack of correlation between the optical and prompt gamma-ray emission, two different processes must have produced the two emission episodes. This is well expected in the internal-external shock model of GRB emission where an external reverse shock arises due to the interaction of the ejecta and the surrounding material. The reverse shock then crosses the emitted shell, thereby accelerating the electrons which then cool adiabatically

(Sari & Piran 1999). This shock occurs only once, hence emitting a single burst.

4. Summary

GRB 0910124 was a very long burst which lasted for $T_{90} \approx 1020$ s. The prompt-ray gamma light curve is characterized by three emission episodes separated by approximately 630 s and 200 s of quiescence, respectively. The optical light curve shows two peaks. The first one occurs well before the onset of the second emission process in gamma-rays. We interpret the first peak as the the reverse shock, thus adding another burst to the sample of GRBs with an optical flash. A more detailed analysis on GRB 091024 has been published by (Gruber et al. 2011).

Acknowledgements. The GBM project is supported by the German Bundesministerium für Wirtschaft und Technologie (BMWi) via the Deutsches Zentrum für Luft- und Raumfahrt (DLR) under the contract numbers 50 QV 0301 and 50 OG 0502. SF acknowledges the support of the Irish Research Council for Science, Engineering and Technology, cofunded by Marie Curie Actions under FP7.

References

- Akerlof et al., C. 1999, *Nature*, 398, 400
 Band et al., D. 1993, *ApJ*, 413, 281
 Beuermann et al., K. 1999, *A&A*, 352, L26
 Bissaldi, E. & Connaughton, V. 2009, *GRB Coordinates Network, Circular Service*, 70
 Burlon et al., D. 2008, *ApJL*, 685, L19
 Cano et al., Z. 2009, *GRB Coordinates Network, Circular Service*, 66
 Evans et al., P. A. 2007, *A&A*, 469, 379
 Evans et al., P. A. 2009, *MNRAS*, 397, 1177
 Gruber et al., D. 2011, *ArXiv e-prints*
 Henden, A., et al. 2009, *GRB Coordinates Network, Circular Service*, 73
 Kobayashi, S. 2000, *ApJ*, 545, 807
 Koshut et al., T. M. 1995, *ApJ*, 452, 145
 Krühler et al., T. 2009a, *ApJ*, 697, 758
 Krühler et al., T. 2009b, *A&A*, 508, 593
 Kumar, P. & Piran, T. 2000, *ApJ*, 535, 152
 Lazzati, D. 2005, *MNRAS*, 357, 722
 Meegan et al., C. 2009, *ApJ*, 702, 791
 Molinari et al., E. 2007, *A&A*, 469, L13
 Oates et al., S. R. 2009, *MNRAS*, 395, 490
 Page, K. L. & Marshall, F. E. 2009, *GRB Coordinates Network, Circular Service*, 69
 Page et al., K. L. 2007, *ApJ*, 663, 1125
 Panaitescu, A. & Vestrand, W. T. 2008, *MNRAS*, 387, 497
 Racusin et al., J. L. 2008, *Nature*, 455, 183
 Rees, M. J. & Meszaros, P. 1998, *ApJL*, 496, L1+
 Sari, R. & Piran, T. 1999, *ApJ*, 520, 641
 Updike et al., A. C. 2009, *GRB Coordinates Network, Circular Service*, 74, 1 (2009), 74
 Vestrand et al., W. T. 2005, *Nature*, 435, 178
 Zhang et al., B. 2006, *ApJ*, 642, 354